Electronic Supplementary Material (ESI) for Analytical Methods.
This journal is © The Royal Society of Chemistry 2024

Supporting Information

Improved *on-line* benchtop ^{31}P NMR reaction monitoring *via* multi resonance SHARPER

Laura Tadiello,[a,b] Meghan E. Halse,[b]* and Torsten Beweries[a]*

a. Leibniz Institute for Catalysis, Albert-Einstein-Str. 29a, 18059 Rostock, Germany; torsten.beweries@catalysis.de
b. Department of Chemistry, University of York, YO10 5DD, York, United Kingdom; meghan.halse@york.ac.uk

Electronic Supplementary Information (ESI)

Experimental details

Low-field NMR spectroscopy

^{31}P NMR spectra have been recorded on a Spinsolve benchtop 80 MHz spectrometer (Magritek), with ^{1}H, ^{19}F detection and an additional channel for the ^{31}P nucleus. Chemical shifts (δ) are reported in parts per million (ppm), internally referenced to the chosen deuterated or non-deuterated solvent. All ^{31}P NMR spectra have been recorded with proton decoupling unless otherwise stated. Shimming has been periodically performed on 90% deuterated water. The spectrometer was purchased together with the reaction monitoring software package (RMX) and a kit for reaction monitoring, containing a glass centering tube (flow cell), a peristaltic pump (BT100-2J, Drifton) and PTFE tubing. Afterwards, the flow setup was modified to our customised setup for inert conditions for highly oxygen-sensitive complexes.[1] Moreover, the Spinsolve software was updated to the latest version (Spinsolve 2.0.0) and the solvent suppression (presaturation sequence) package was included. Finally, to create and manipulate the SHARPER sequences, the Spinsolve Expert software was used (version 1.41.22). According to the supplier, the flow NMR cell can be operated with a pressure of up to 10 bar. Regarding the temperature, the limits are reported to be 20–25 °C, with a tolerable fluctuation of ± 2 °C.

Materials

[Rh((*R,R*)-DIPAMP)(NBD)]BF_4 (Umicore, 100%) was transferred to a Schlenk flask and kept under inert atmosphere. The non-deuterated solvent used (*i.e.*, MeOH) were distilled under argon and stored in burettes under inert atmosphere. The deuterated solvent used (*i.e.*, DCM-d_2) was distilled under argon and afterwards the freeze-pump-thaw method was applied.

Analysis via MestReNova (for all NMR spectra)

All NMR spectra were analysed *via* Mestrenova (Mestrelab Research, version 14.3.2). Manual baseline correction and phase correction were preferred to the corresponding automatic ones. In the case of ^{31}P NMR, apodisation was typically applied, typically with exponential line broadening. Zero filling was also applied, if considered appropriate.

The data analysis tool of MestReNova was used for reaction monitoring after applying phase correction, baseline correction, zero filling and apodisation in stack mode.

Analysis via MestReNova (specifically for SHARPER spectra)

Most of the SHARPER spectra required first order phase correction (PH1) in addition to the zero order phase correction (PH0) because of the consequences of the FID truncation.

Analysis via Origin

All kinetic profiles were analysed *via* Origin (OriginLab Corporation, version 10.0.5.157). Plots showing the evolution of the normalised integral values over time were obtained by normalising for the number of nuclei and the total amount of active nuclei. The exponential fits were calculated for a better visualisation of the data.

Preparation (for static and flow conditions)

All manipulations were carried out using standard Schlenk techniques under oxygen- and moisture-free conditions. Inert conditions were achieved performing at least six vacuum/argon cycles. Hydrogenation reactions were conducted under 1.3–1.5 bar of hydrogen, supplied directly into the fume hood from a central line available at LIKAT.

Preparation (specifically for flow conditions)

For all experiments under flow conditions, the entire setup was rigorously cleaned, dried as well as evacuated and back-filled with argon multiple times (more time for these cycles is require in flow compared to static conditions). Flow calibration was performed. Before starting the reaction monitoring, the solution was pumped from the reaction vessel into the flow system at the double of the speed used during reaction monitoring, only for the first minute. This was required to help the pump to push the solution against the argon present in the flow.

General definitions & abbreviations

Definitions used in the publication

The term “loop” used in the context of reaction monitoring, is defined in this publication as the group of experiments that are repeated multiple times. One loop might contain a $^{31}P\{^{1}H\}$ NMR sequence or a MR-SHARPER ^{31}P NMR sequence or both.

Abbreviations used in the tables

Total number of points (TP); number of points (NP); dwell time (DW); number of scans (NS); acquisition time (AT); repetition time (RT); removed points (RP); imaginary part not removed from FID (RI0) *vs* imaginary part removed from FID (RI1); homospoil amplitude (HA); homospoil duration (HD); acquisition delay (AD); echo time (ET); chunk length (CL).

SHARPER sequences

As overview and additional guide, we report here the key points of the SHARPER sequence.

Figure S1 illustrates the SHARPER sequence.[2] The first non-selective 90° pulse (A) brings the magnetisation into the transversal plane. Then, a first free induction decay (FID) chunk is acquired (B). Please note that this is called "half chunk" because it is acquired for half of the time of the following FID chunks. The refocusing loop follows and it consists of a chain of 180° pulses (C) alternated by FID chunks acquisitions (D). The final FID, obtained after processing, brings together all the FID chunks reordered. Since each FID chunk is very short, there is no time for J-coupling evolution and therefore for the formation of the multiplet. Moreover, the refocusing loop eliminates the effects of field inhomogeneity.

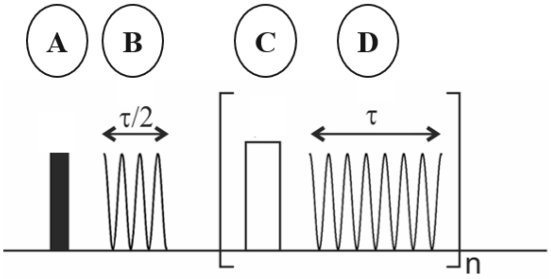

Figure S1. Schematic view of SHARPER pulse sequence.[3] The non-selective 90° (A) and 180° pulse (C) are depicted as rectangles. The first FID chunk (B) is acquired for half the acquisition time (τ/2) while the FID chunks (D) in the refocussing loop are acquired for full acquisition time (τ).

The SHARPER sequence as visualised by the Spinsolve Expert software is reported (Figure S2). After technical settings relevant for the spectrometer, the Waltz sequence is applied on the proton channel to produce the nuclear Overhauser effect (NOE, A). After a delay, the non-selective 90° pulse (B) is applied to bring the magnetisation into the *XY* plane. After a delay, the FID half chunk is acquired (C). The refocusing loop follows, characterised by the non-selective 180° pulse (E) surrounded by delays (D, F) and the FID chunk (G). The pulse gated overheat (pgo) and receiver latency (rxLat) values are delays due to the electronics in the spectrometer. The first corresponds to a delay before a pulse while the second refers to a delay before the acquisition of the FID. Echo time (ET) is here defined as the delay that precedes and follows the 180° pulse (corrected accordingly with the pgo or rxLat parameter). The chunk length (CL) corresponds to the acquisition time of the various FID chunks inside the refocussing loop. The last repetition (H) is included if required to acquire the correct total number of points entered by the user.

The sel-SHARPER sequence is also reported (Figure S3).[3] The new aspects, compared to SHARPER, are the following: the non-selective 90° pulse is replaced by a selective spin echo element, containing a Gaussian 180° pulse (J) surrounded by gradients (I, K). Three selective pulses, all shaped as Gaussian but with different selectivity, have been screened (Figure S4). As explicitly indicated, the gradients are applied along the three dimensions (*X*, *Y* and *Z*). The first gradient (I) and the second one (K) have the same phase. In this way, the magnetisation that is inverted by the selective Gaussian pulse is refocussed while the one that is outside of the range gets even more dephased.

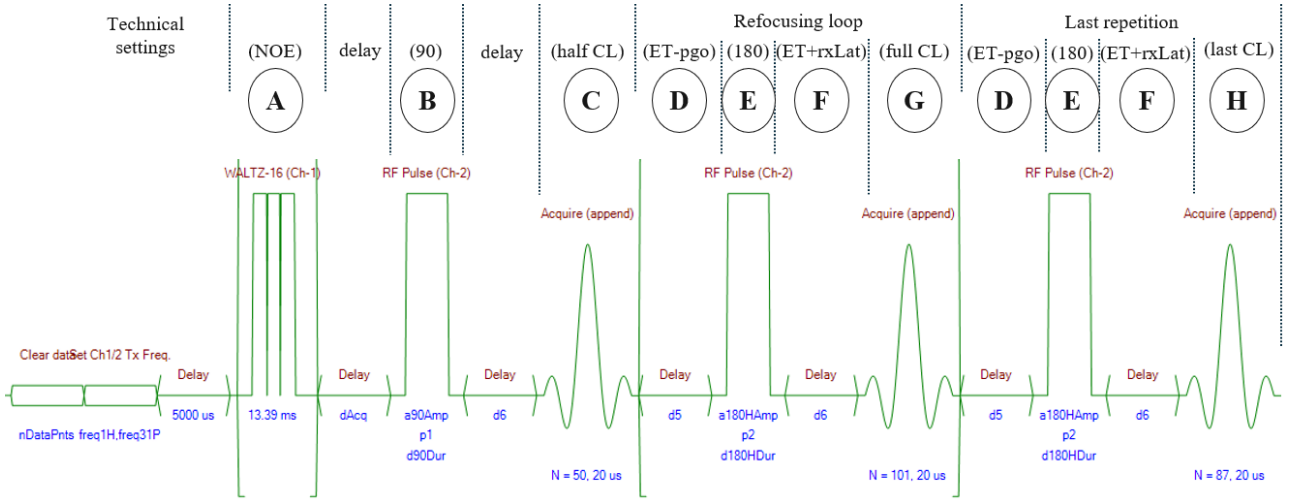

Figure S2. SHARPER sequence as visualised in Spinsolve Expert. Additional comments to guide the reader are shown in black.

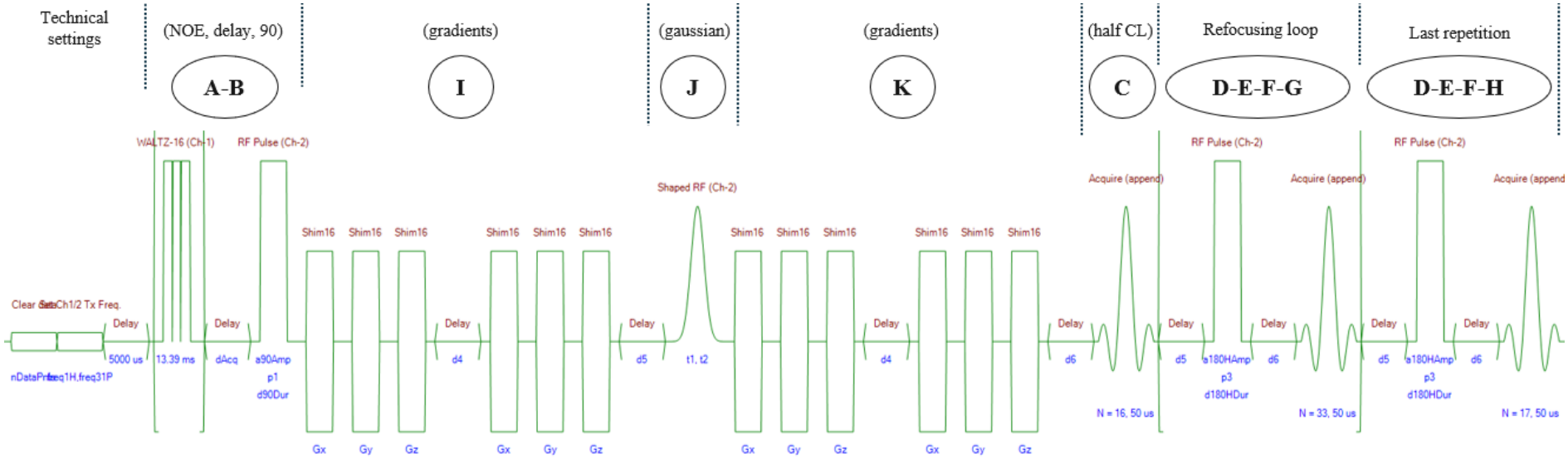

Figure S3. Sel-SHARPER sequence as visualised in Spinsolve Expert. Additional comments to guide the reader are shown in black.

It has been demonstrated previously that if appropriate phasing of the time domain data is achieved, removal of the imaginary part prior to Fourier transformation can improve the SNR by an additional factor of 1.4.[4] In the results presented here, phasing was applied in post-processing and the imaginary part was not removed. In principle, a further increase in the SNR enhancements could be achieved by adjusting the acquisition parameters to achieve appropriate time domain phasing allowing for the removal of the imaginary part prior to Fourier transformation.

Within the automatic processing that reconstructs the full FID from the data chunks, we typically removed one point from the start of each chunk to obtain a smoother FID transition between chunks and minimise artefacts. In principle, the delay between the 180° pulses and the start of the data acquisition could be adjusted to minimise the discontinuity between successive chunks; however, we found in practice that removing the first point from each chunk in post-processing was the most effective way to minimise artefacts.

With a strong J_{RhP} coupling of 140–210 Hz, as in the Rh(I) DIPAMP systems used herein, only relatively short chunk lengths are allowed (*ca.* 2 ms). A longer chunk length will allow the scalar coupling to evolve and therefore the multiplet will not fully collapse into a singlet. However, a shorter chunk length will reduce the effective acquisition time (due to the time required for the more frequent refocusing pulses) and therefore reduces the SNR enhancement.

We have added the NOE part to the SHARPER sequence for ^{31}P nucleus, gaining a comparable increase in SNR to that observed in the ^{31}P{^{1}H} spectra (Figure S5). A key point consisted in merging the phase cycle of traditional ^{31}P sequence with NOE and the phase of the SHARPER sequence (Table S1).

Table S1. Phases cycling lists for the described sequences.

Sequence	**Phases list**	**Comments**
traditional ^{31}P{^{1}H} with NOE	[0,2,0,2; 0,0,2,2; 2,2,0,0; 0,2,0,2]	90 pulse (p1) NOE and decoupling (p2) NOE and decoupling (p3) acquisition (p4)
SHARPER ^{31}P without NOE	[0,0,2,2,1,1,3,3; 3,1,3,1,2,0,2,0; 0,0,2,2,1,1,3,3]	90 pulse (p1) 180 pulse (p2) acquisition (p3)
SHARPER ^{31}P with NOE	[0,2,0,2; 3,1,3,1; 0,0,2,2; 2,2,0,0; 0,2,0,2]	90 pulse (p1) 180 pulse (p2) NOE (p3) NOE (p4) acquisition (p5)
sel-SHARPER ^{31}P without NOE	[0,0,2,2,1,1,3,3; 1,3,1,3,0,2,0,2; 3,1,3,1,2,0,2,0; 0,0,2,2,1,1,3,3]	90 non-selective pulse (p1) 180 selective pulse (p2) 180 non-selective pulse (p3) acquisition (p4)
sel-SHARPER ^{31}P with NOE	[0,2,0,2; 1,3,1,3; 3,1,3,1; 0,0,2,2; 2,2,0,0; 0,2,0,2]	90 non-selective pulse (p1) 180 selective pulse (p2) 180 non-selective pulse (p3) NOE (p4) NOE (p5) acquisition (p6)

Pulses calibrations

The calibrated values for the non-selective 90° pulse were 13 µs and 67 µs, respectively for ^{1}H and ^{31}P nuclei (water and KH_2PO_4 were used as samples).

Single Pulsed Field Gradient (SPFG) spin echo sequences were used for calibration of selective pulses. Amplitude and offset sweeps were realised (Figure S4) to obtain respectively optimal power and selectivity (in terms of FWHM) of the three Gaussian with chosen durations of the pulse (*i.e.*, 10 ms, 5 ms and 3 ms). As expected, the Gaussian pulse with the longest duration (duration of 10 ms) requires the lowest power (power of -37.5 dB) and is the one with the smallest FWHM (FWHM of 4.79 ppm) which corresponds to the most selective pulse.

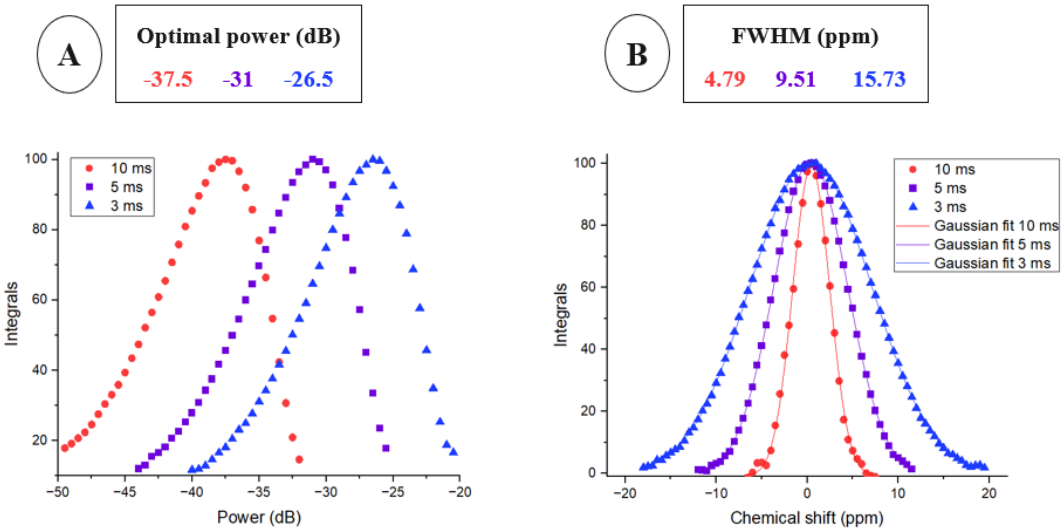

Figure S4. ^{31}P SPFG spin echo of KH_2PO_4 in water. The amplitude sweep allows the determination of the optimal power (A) while the offset sweep allows the determination of the selectivity (B). Please note that the chemical shift on the horizontal axis is set to zero at the centre of the peak.

Single-component solution

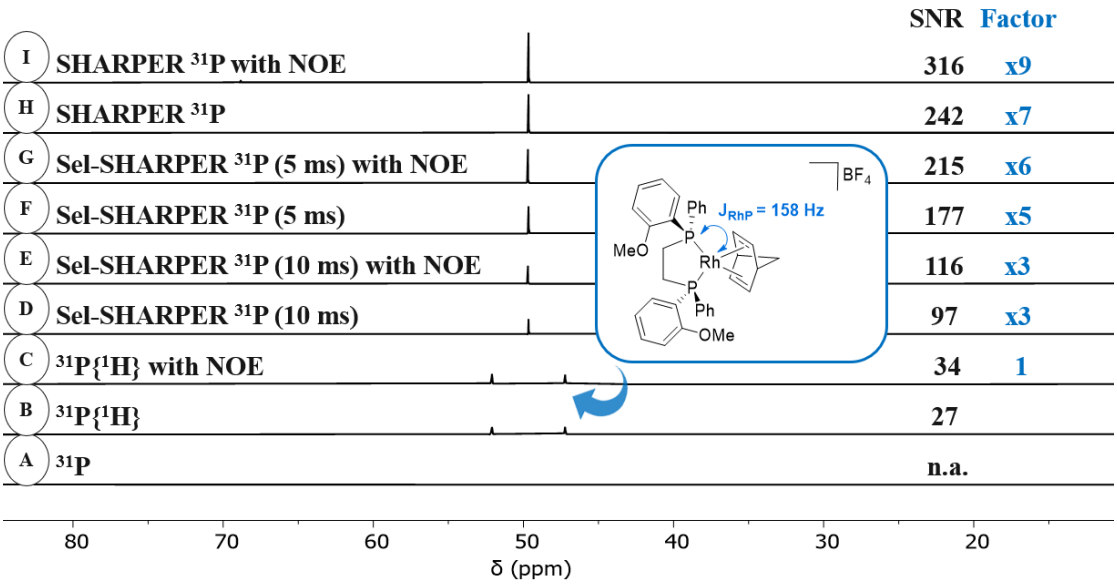

Figure S5. Expansion of Figure 1 for better visualisation. Comparison between ^{31}P NMR and SHARPER experiments of [Rh((*R,R*)-DIPAMP)(NBD)]BF_4 (112 mM in DCM-d_2): ^{31}P NMR spectrum without decoupling from ^{1}H and without NOE (A); ^{31}P{^{1}H} NMR spectra, with or without NOE (B,C); sel-SHARPER ^{31}P NMR spectra with a Gaussian-shaped selective pulse of the duration of 10 ms, with or without NOE (D,E); sel-SHARPER ^{31}P NMR spectra with a Gaussian-shaped selective pulse of the duration of 5 ms, with or without NOE (F,G); SHARPER ^{31}P NMR spectra, with or without NOE (H,I). Please refer to Figure S6 for off-resonance behaviour analysis.

Table S2. Experimental and processing parameters of Figure S5, expansion of Figure 1.

	Experimental parameters										Processing parameters					
#	Offset (ppm)	TP	NP	DW (µs)	NS	AT (s)	CL (ms)	RT (s)	Exp. time	Others	Zero filling	Exp. Apod. (Hz)	Noise Region (ppm)	Peak Region (ppm)	SNR	Factor
I	49.66	66k	16	50	8	-	1.6	25	2min58s	RP1 RI0	2 (128K)	0.2	100-200	49-50	316	9
H	49.66	66k	16	50	8	-	1.6	25	2min58s	RP1 RI0	2 (128K)	0.2	100-200	49-50	242	7
G	49.7	66k	16	50	8	-	1.6	25	2min58s	gaussian 5ms -31dB; HA10k, HD600us; AD50us; RP1 RI0	2 (128K)	0.2	100-200	49-50	215	6
F	49.66	66k	16	50	8	-	1.6	25	2min58s	gaussian 5ms -31dB; HA10k, HD600us; AD50us; RP1 RI0	2 (128K)	0.2	100-200	49-50	177	5
E	49.7	66k	16	50	8	-	1.6	25	2min58s	gaussian 10ms -37.5dB; HA10k, HD600us; AD50us; RP1 RI0	2 (128K)	0.2	100-200	49-50	116	3
D	49.66	66k	16	50	8	-	1.6	25	2min58s	gaussian 10m -37.5dB; HA10k, HD600us; AD50us; RP1 RI0	2 (128K)	0.2	100-200	49-50	97	3
C	50	-	66k	25	8	1.7	-	15	1min50s	-	2 (128K)	0.2	100-200	46-53	34	1
B	37	-	66k	25	8	1.7	-	15	1min50s	-	2 (128K)	0.2	100-200	46-53	27	-
A	37	-	66k	25	8	1.7	-	15	1min50s	-	2 (128K)	0.2	100-200	46-53	n.a.	-

Off-resonance behaviour of a single-component solution

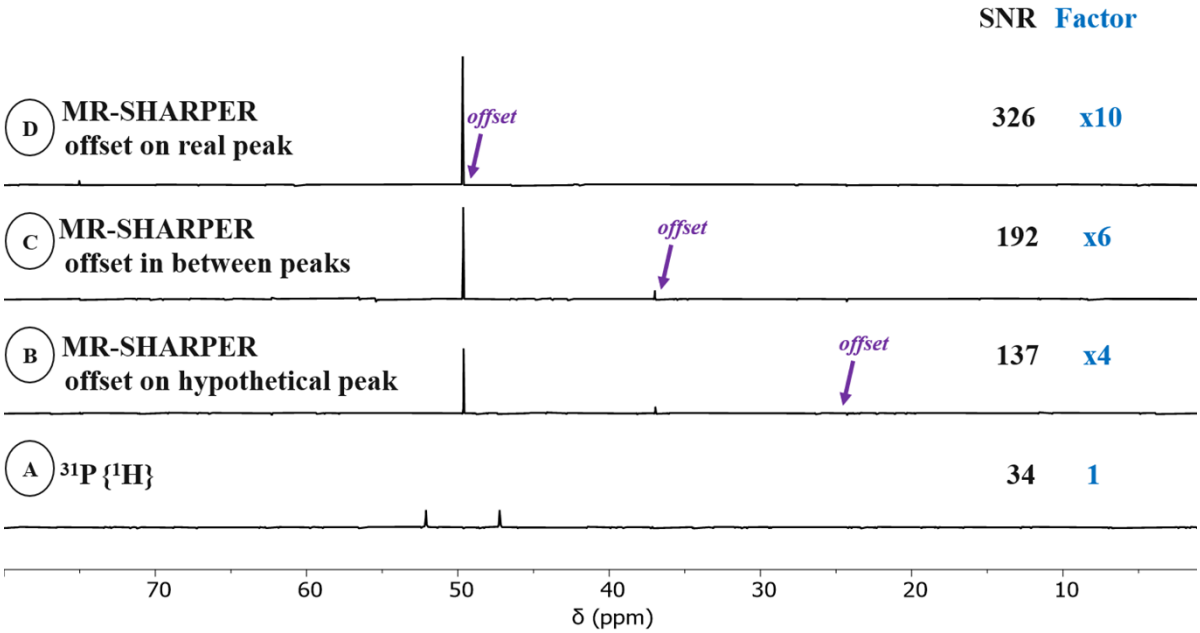

Figure S6. Comparison between $^{31}P\{^{1}H\}$ NMR and MR-SHARPER experiments of [Rh((*R,R*)-DIPAMP)(NBD)]BF_4 (112 mM in DCM-d_2): $^{31}P\{^{1}H\}$ NMR spectrum with NOE (A); MR-SHARPER ^{31}P NMR spectrum with NOE and offset on hypothetical peak at 24.27 ppm (B); MR-SHARPER ^{31}P NMR spectrum with NOE and offset in between hypothetical and real peak at 35.97 ppm (C); MR-SHARPER ^{31}P NMR spectrum with NOE and offset on real peak at 49.67 ppm (D).

Table S3. Experimental and processing parameters of Figure S6.

	Experimental parameters										Processing parameters								
#	Offset (ppm)	TP	NP	DW (µs)	NS	AT (s)	CL (ms)	RT (s)	Exp. time	Others	Zero filling	Exp. Apod. (Hz)	Noise Region (ppm)	Peak Region (ppm)	SNR	Factor	Peak region´ (ppm)	SNR´	Factor´
D	49.67	66k	11	55	8	-	1.21	25	2min58s	RP1 RI0	2 (128K)	0.2	100-200	49-50	326	10	-	-	-
C	36.97	66k	22	55	8	-	2.42	25	2min58s	RP1 RI0	2 (128K)	0.2	100-200	49-50	192	6	-	-	-
B	24.27	66k	22	55	8	-	2.42	25	2min58s	RP1 RI0	2 (128K)	0.2	100-200	49-50	137	4	-	-	-
A	50	-	66k	50	8	3.3	-	15	1min50s	-	2 (128K)	0.2	100-200	46-53	34	1	-	-	-

Two-component solution

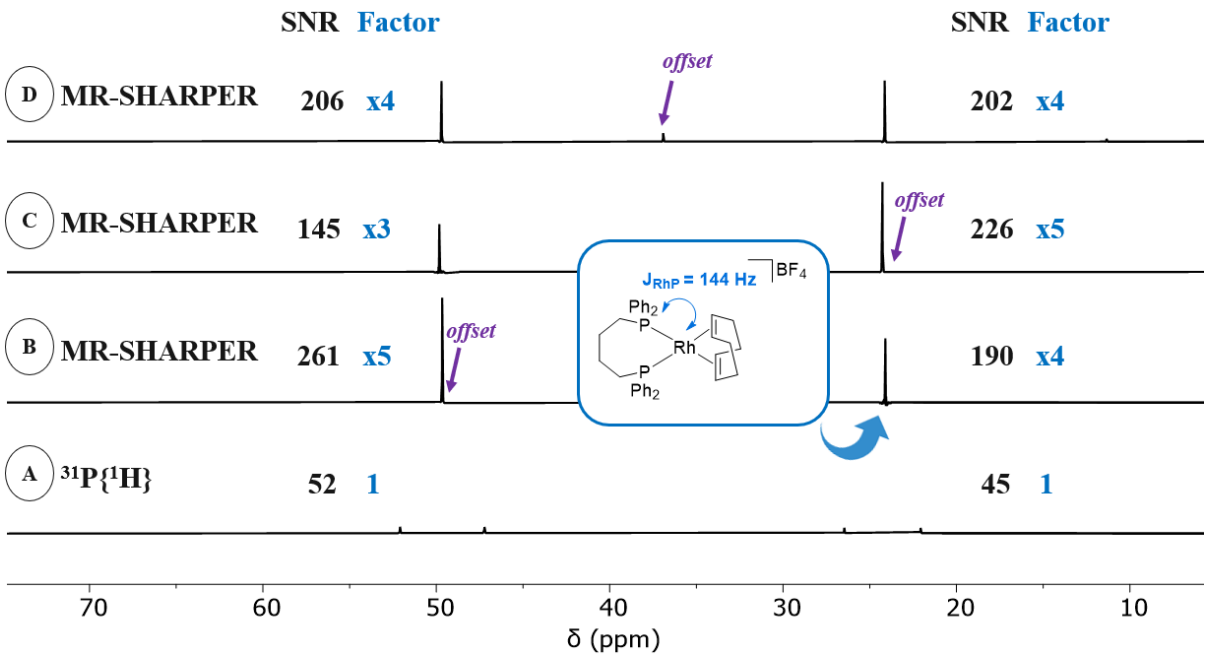

Figure S7. Comparison between $^{31}P\{^{1}H\}$ NMR and MR-SHARPER experiments of a mixture of [Rh((*R,R*)-DIPAMP)(NBD)]BF_4 (107 mM in DCM-d_2) and [Rh(DPPB)(COD)]BF_4 (106 mM in DCM-d_2): $^{31}P\{^{1}H\}$ NMR spectrum with NOE (A); MR-SHARPER ^{31}P NMR spectrum with NOE and offset on peak at 49.66 ppm (B); MR-SHARPER ^{31}P NMR spectrum with NOE and offset on peak at 24.27 ppm (C); MR-SHARPER ^{31}P NMR spectrum with NOE and offset in between peaks at 36.92 ppm (D).

Table S4. Experimental and processing parameters of Figure S7.

	Experimental parameters										Processing parameters								
#	Offset (ppm)	TP	NP	DW (µs)	NS	AT (s)	CL (ms)	RT (s)	Exp. time	Others	Zero filling	Exp. Apod. (Hz)	Noise Region (ppm)	Peak Region (ppm)	SNR	Factor	Peak region´ (ppm)	SNR´	Factor´
D	36.92	66k	60	20	8	-	2.4	25	2min58s	RP1 RI0	4 (256K)	0.3	100-200	49-50	206	4	23.5-24.5	202	4
C	24.27	66k	40	15	8	-	1.2	25	2min58s	RP1 RI0	4 (256K)	0.3	100-200	49-50	145	3	23.5-24.5	226	5
B	49.66	66k	40	15	8	-	1.2	25	2min58s	RP1 RI0	4 (256K)	0.3	100-200	49-50	261	5	23.5-24.5	190	4
A	37	-	66k	-	8	3.3	-	15	1min50s	-	4 (256K)	0.3	100-200	46-53	52	1	20-28	45	1

Comparison considering same number of scans *vs* same experiment time

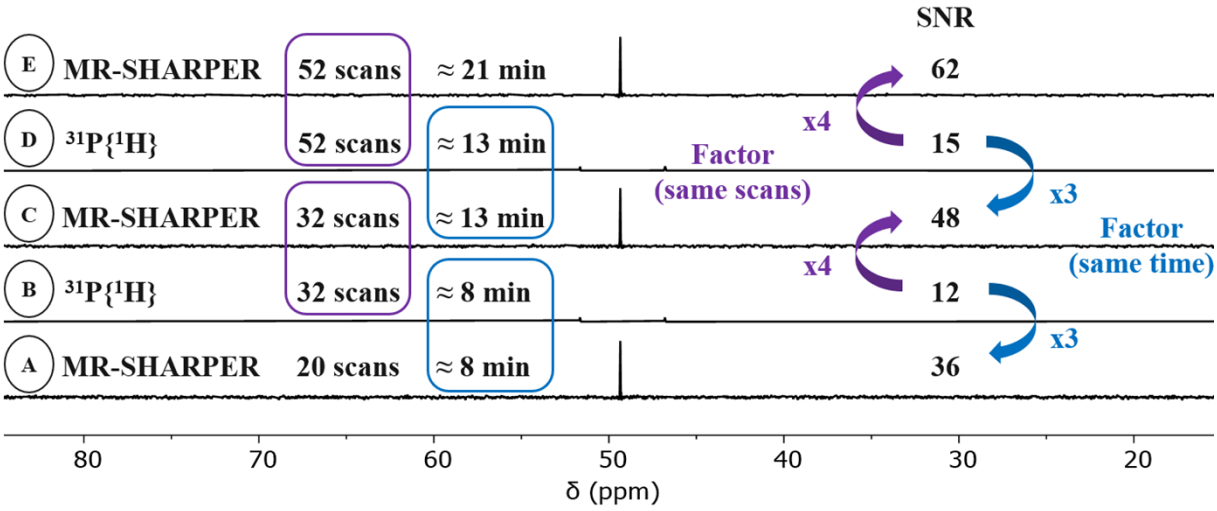

Figure S8. Comparison between $^{31}P\{^{1}H\}$ NMR and MR-SHARPER experiments of a mixture of [Rh((*R,R*)-DIPAMP)(NBD)]BF_4 (9 mM in MeOH): $^{31}P\{^{1}H\}$ NMR spectra with NOE (B,D); MR-SHARPER ^{31}P NMR spectra with NOE (A,C,E).

Table S5. Experimental and processing parameters of Figure S8.

	Experimental parameters										Processing parameters								
#	Offset (ppm)	TP	NP	DW (µs)	NS	AT (s)	CL (ms)	RT (s)	Exp. time	Others	Zero filling	Exp. Apod. (Hz)	Noise Region (ppm)	Peak Region (ppm)	SNR	Factor	Peak region´ (ppm)	SNR´	Factor´
E	64.56	66k	72	14	52	-	2.02	25	21min19s	RP1 RI0; ET20	2 (128K)	0.3	100-200	49-50	62	-	-	-	-
D	65	-	66k	50	52	3.3	-	15	12min51s	-	2 (128K)	0.3	100-200	46-53	15	-	-	-	-
C	64.56	66k	72	14	32	-	2.02	25	13min0s	RP1 RI0; ET20	2 (128K)	0.3	100-200	49-50	48	-	-	-	-
B	65	-	66k	50	32	3.3	-	15	7min50s	-	2 (128K)	0.3	100-200	46-53	12	-	-	-	-
A	64.56	66k	72	14	20	-	2.02	25	7min59s	RP1 RI0; ET20	2 (128K)	0.3	100-200	49-50	36	-	-	-	-

Reaction monitoring in static conditions (≈ 8 min / spectrum)

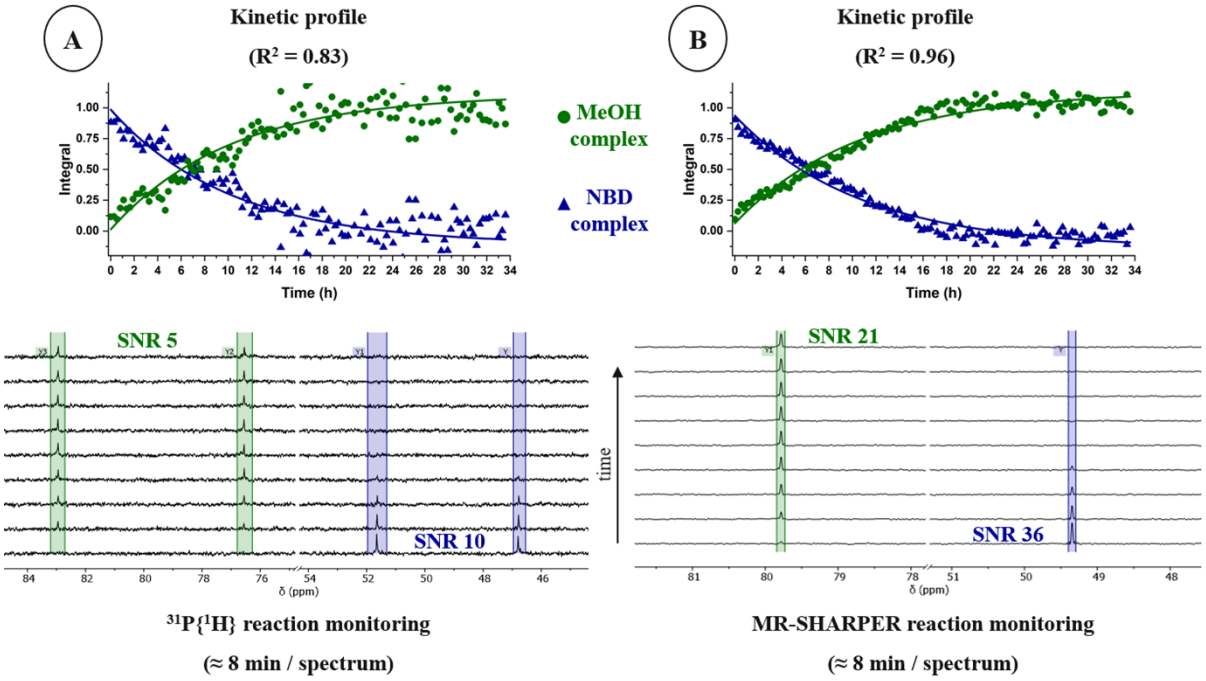

Figure S9. Comparison between $^{31}P\{^{1}H\}$ NMR (A) and MR-SHARPER (B) reaction monitoring (9 mM in MeOH) of the hydrogenation of [Rh((*R,R*)-DIPAMP)(NBD)]BF_4 to produce [Rh((*R,R*)-DIPAMP)$(MeOH)_2$]BF_4 (Scheme 1).

Details. Reaction monitoring with 124 loops, characterised by: $^{31}P\{^{1}H\}$ NMR (32 scans; 3.3 s acquisition time; 15 s repetition time; 7 min 50 s experiment time); MR-SHARPER ^{31}P NMR (20 scans; 2.02 ms chunk length; 25 s repetition time; 7 min 59 s experiment time). Each loop lasted 17 min 1 s. For clarity, only one spectrum every 15th is shown.

Table S6. Experimental and processing parameters of Figure S9.

	Experimental parameters										Processing parameters								
#	Offset (ppm)	TP	NP	DW (µs)	NS	AT (s)	CL (ms)	RT (s)	Exp. time	Others	Zero filling	Exp. Apod. (Hz)	Noise Region (ppm)	Peak Region (ppm)	SNR	Factor	Peak region´ (ppm)	SNR´	Factor´
B	65	-	66k	50	32	3.3	-	15	7min50s	-	4 (256K)	0.3	100-200	46-53	10	-	manual selection	5	-
A	64.56	66k	72	14	20	-	2.02	25	7min59s	RP1 RI0; ET20	4 (256K)	0.3	100-200	49-50	36	4	79-80	21	4

Reaction monitoring in static conditions (≈ 1 min / spectrum)

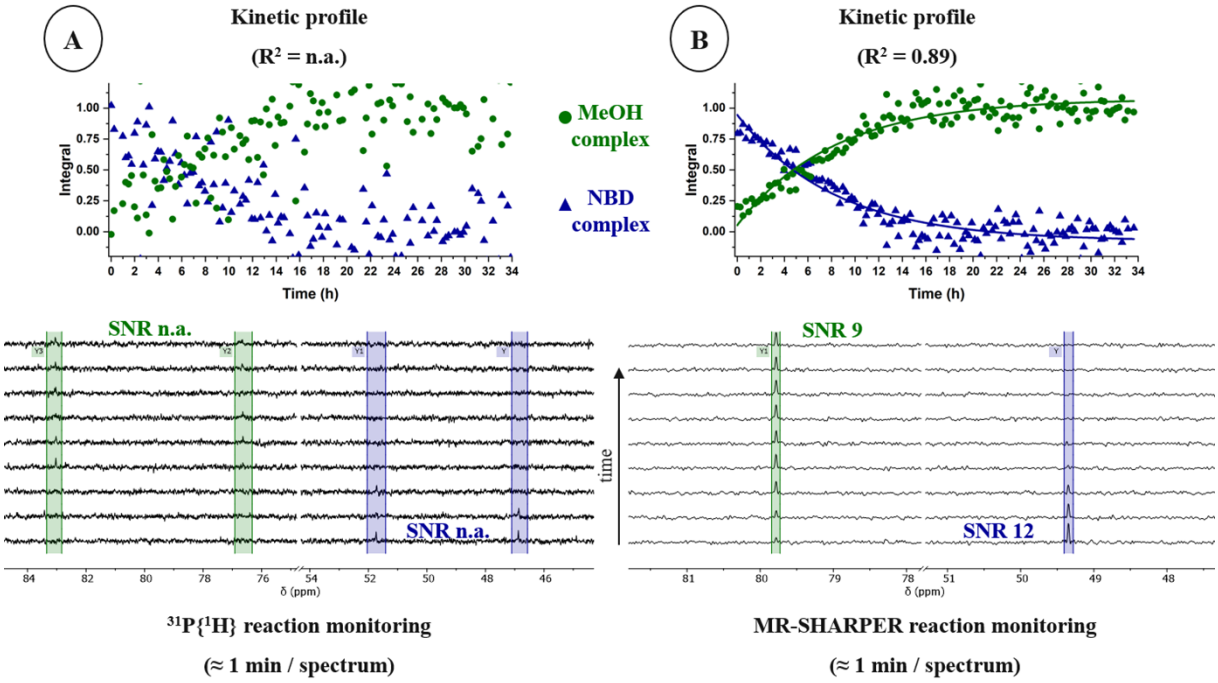

Figure S10. Comparison between $^{31}P\{^{1}H\}$ NMR (A) and MR-SHARPER (B) reaction monitoring (9 mM in MeOH) of the hydrogenation of $[Rh((R,R)\text{-DIPAMP})(NBD)]BF_4$ to produce $[Rh((R,R)\text{-DIPAMP})(MeOH)_2]BF_4$ (Scheme 1).

Details. Reaction monitoring with 124 loops, characterised by: $^{31}P\{^{1}H\}$ NMR (4 scans; 3.3 s acquisition time; 15 s repetition time; 51 s experiment time); MR-SHARPER ^{31}P NMR (3 scans; 2.02 ms chunk length; 25 s repetition time; 54 s experiment time). Each loop lasted 16 min 58 s (additional delay has been added to compare with the reaction monitoring in Figure S9). For clarity, only one spectrum every 15th is shown.

Table S7. Experimental and processing parameters of Figure S10.

	Experimental parameters										Processing parameters								
#	Offset (ppm)	TP	NP	DW (µs)	NS	AT (s)	CL (ms)	RT (s)	Exp. time	Others	Zero filling	Exp. Apod. (Hz)	Noise Region (ppm)	Peak Region (ppm)	SNR	Factor	Peak region´ (ppm)	SNR´	Factor´
B	65	-	66k	50	4	3.3		15	51s	-	4 (256K)	0.3	100-200	46-53	n.a.	-	76-84	n.a.	-
A	64.56	66k	72	14	3	-	2.02	25	54s	RP1 RI0; ET20	4 (256K)	0.3	100-200	49-50	12	n.a.	79-80	9	n.a.

Reaction monitoring in flow conditions (≈ 1 min / spectrum)

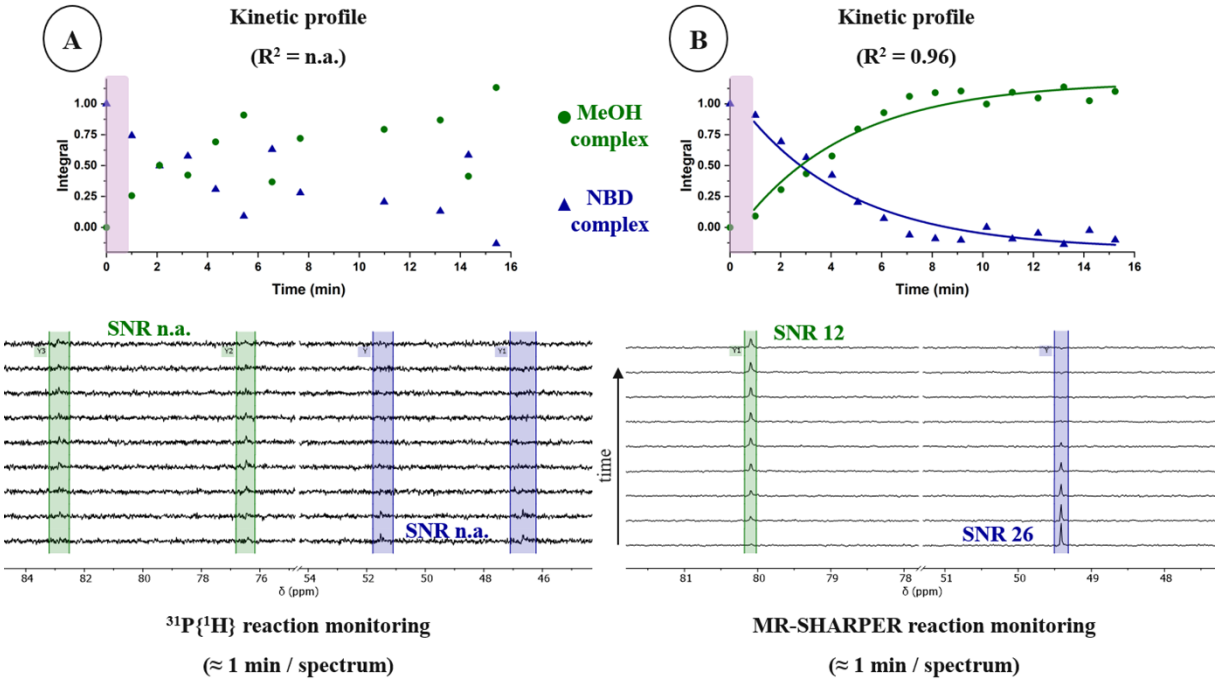

Figure S11. Comparison between $^{31}P\{^{1}H\}$ NMR (A) and MR-SHARPER (B) reaction monitoring (30 mM in MeOH) of the hydrogenation of $[Rh((R,R)\text{-DIPAMP})(NBD)]BF_4$ to produce $[Rh((R,R)\text{-DIPAMP})(MeOH)_2]BF_4$ (Scheme 1). In purple is highlighted the preparation time. The two points in each kinetic profile appearing at time zero has been taken from the spectra ($^{31}P\{^{1}H\}$ NMR and MR-SHARPER ^{31}P NMR) in flow conditions of the starting material.

Details. The first reaction monitoring with 9 loops, characterised by: $^{31}P\{^{1}H\}$ NMR (10 scans; 1.6 s acquisition time; 6 s repetition time; 59 s experiment time). The second reaction monitoring with 9 loops, characterised by: MR-SHARPER ^{31}P NMR (7 scans; 2.0 ms chunk length; 9 s repetition time; 58 s experiment time). Each loop lasted 59 s for $^{31}P\{^{1}H\}$ NMR and 58 s for MR-SHARPER ^{31}P NMR reaction monitoring.

Table S8. Experimental and processing parameters of Figure S11.

	Experimental parameters										Processing parameters								
#	Offset (ppm)	TP	NP	DW (µs)	NS	AT (s)	CL (ms)	RT (s)	Exp. time	Others	Zero filling	Exp. Apod. (Hz)	Noise Region (ppm)	Peak Region (ppm)	SNR	Factor	Peak region´ (ppm)	SNR´	Factor´
B	65	-	66k	25	10	1.6	-	6	59s	flow	2 (128K)	0.2	100-200	46-53	n.a.	-	76-84	n.a.	-
A	64.75	66k	50	20	7	-	2.02	9	58s	RP1 RI0; ET20; flow	2 (128K)	0.2	100-200	49-50	26.2	-	79.5-80.5	11.9	-

References

1 L. Tadiello, H.-J. Drexler and T. Beweries, *Organometallics,* 2022, **41**, 2833-2843.

2 A. B. Jones, G. C. Lloyd-Jones and D. Uhrín, *Anal. Chem.,* 2017, **89**, 10013-10021.

3 A. I. Silva Terra, M. Rossetto, C. L. Dickson, G. Peat, D. Uhrín and M. E. Halse, *ACS Meas. Sci. Au,* 2023, **3**, 73-81.

4 C. L. Dickson, G. Peat, M. Rossetto, M. E. Halse and D. Uhrín, *Chem. Commun.,* 2022, **58**, 5534-5537.